Charge state effect on the K-shell ionization of iron by xenon ions near the Bohr velocity*

Zhou Xian-Ming(周贤明)[a], Zhao Yong-Tao(赵永涛)[a]†, Ren Jie-Ru(任洁茹)[a,b], Cheng Rui(程 锐)[a], Lei Yu(雷 瑜)[a], Sun Yuan-Bo(孙渊博)[a], Xu Ge(徐 戈)[a,b], Wang Yu-Yu(王瑜玉)[a], Liu Shi-Dong(刘世东)[a,b], and Xiao Guo-Qing(肖国青)[a]

[a] *Institute of Modern Physics, Chinese Academy of Sciences, Lanzhou* 730000, *China*
[b] *University of Chinese Academy of Sciences, Beijing* 100049, *China*

(Received 27 March 2013; revised manuscript received 15 May 2013)

Fe K-shell ionization cross sections induced by 2.4–6.0 MeV Xe^{20+} are measured and compared with different binary-encounter-approximation (BEA) models. The results indicate that the BEA model corrected both by the Coulomb repulsion and by the effective nuclear charge ($Z_{\rm eff}$) agrees well with the experimental data. Comparison of Fe K-shell X-ray emission induced by 5 MeV xenon ions with different initial charge states (20+, 22+, 26+, 30+) verifies the applicability of the effective nuclear charge ($Z_{\rm eff}$) correction for the BEA model. It is found that $Z_{\rm eff}$ correction is reasonable to describe direct ionization induced by xenon ions with no initial M-shell vacancies. However, when the M shell is opened, the $Z_{\rm eff}$ corrected BEA model is unable to explain the inner-shell ionization, and the electron transfer by molecular-orbital promotion should be considered.

Keywords: highly charged ions, charge state effect, inner-shell ionization, X-ray emission

PACS: 34.80.Dp, 32.30.Rj, 32.80.Aa **DOI:** 10.1088/1674-1056/22/11/113402

1. Introduction

The interaction of highly charged ions with solids has attracted substantial attention and has been studied both theoretically and experimentally.[1–5] When such ions enter into solid matter, they deposit energy in collisions with target electrons and nuclei. The inner-shell electrons are ionized and the corresponding vacancies de-excite by X-ray emission or Auger transition.[6,7] Investigation of the X-ray emission provides a useful method to study the atomic properties and dynamic mechanisms of ion–solid collisions.[8]

Direct ionization (DI),[9] electron capture (EC),[10] and electron transfer via molecular-orbital (MO) promotion[11] are the three basic channels of inner-shell ionization in ion–atom collision. It is well known that DI is the predominant mechanism for the strongly asymmetric and fast collision where $Z_1 \ll Z_2$ and $v_{\rm p}/v_i \gg 1$, with Z_1 and Z_2 being the respective atomic numbers of the incident ion and the target atom, $v_{\rm p}$ the velocity of the projectile, and v_i the orbital velocity of the i-shell electron. For the less asymmetric collision for $Z_1 \leq Z_2$ and $v_{\rm p}/v_i \geq 1$, EC becomes important, and the MO comes into play in the symmetric and very slow collisions for $Z_1 \approx Z_2$ and $v_{\rm p}/v_i \ll 1$.[12] However, the process is still not well understood for the asymmetric and slow collisions with $Z_1 > Z_2$ and $v_{\rm p}/v_i \ll 1$, and the corresponding theoretical and experimental database is small.[13–15] During the slow collisions for highly charged ions near the Bohr velocity ($v_0 = 2.19 \times 10^6$ m/s), the projectile motion of the system is usually slower than that of the orbital electrons, so the collision partners have enough time to adjust their orbits, and inner-shell vacancies may be produced by electron transfer, except for direct Coulomb ionization. Besides, for a thick target, there exists the so-called solid effect, which means that the collision frequency is high compared to the lifetime of the excited states and the charge state equilibrium in solid is reached on the femtosecond timescale.[16] Therefore, there are two contributions to the total X-ray yield, namely, pre-equilibrium and equilibrium emission. The pre-equilibrium emission depends on the initial charge state, and the equilibrium emission, by definition, depends only on the projectile velocity. Several experiments have been devoted to investigating the charge state dependence of the energy loss of slow, highly charged ions in solid, gas, and plasmas,[17–21] and an enhancement of the energy loss with increasing initial charge was observed. Another question related to this research is how the inner-shell ionization of the target atom responds to the change of the initial charge state of the projectile.

The present work aims to modify the original binary-encounter-approximation (BEA) model by effective nuclear charge for inner-shell direct ionization produced by highly charged ions near the Bohr velocity in the asymmetric collisions of $Z_1 > Z_2$. We measured iron K-shell ionization cross section by highly charged heavy Xe^{20+} ions with velocity of $0.86v_0$–$1.36v_0$ and compared the data with the BEA theoreti-

*Project supported by the National Basic Research Program of China (Grant No. 2010CB832902) and the National Natural Science Foundation of China (Grant Nos. 11275241, 11205225, 11105192, and 11275238).

†Corresponding author. E-mail: zhaoyt@impcas.ac.cn

© 2013 Chinese Physical Society and IOP Publishing Ltd

cal approach. Furthermore, we measured the X-ray emission by 5 MeV xenon ions with the initial charge states of 20+, 22+, 26+, and 30+. The particular emphasis will be laid on the dependence of the conception of effective nuclear charge on the initial charge state of the projectile.

2. Experimental methods

The experimental setup is similar to that described in Ref. [22]. The slow, highly charged xenon ions were extracted from the electron cyclotron resonance (ECR) ion source at the Institute of Modern Physics, Chinese Academy of Sciences in Lanzhou. The ion beam was injected into the ultrahigh vacuum target chamber (10^{-8} mbar) by deflection magnet, focusing quadruple magnet, and collimation diaphragm. The beam impacted perpendicularly onto the target surface. The diameter of the beam spot was about 3 mm. The emitted X rays were detected by a silicon drift detector (SDD) at 45° with respect to the beam direction and with a geometrical solid angle of 0.0066 sr. The detector has an energy resolution of about 136 eV at 5.9 keV and effective energy range of 0.5 keV–14 keV when the gain was selected as 100, and the efficiency has been given by the manufacturers. We note the beam was not measured directly. Instead, the projectile current was measured indirectly by combined use of a penetrable Faraday cup and a common Faraday cup for eliminating the influence of the secondary electrons emission. The iron target had a purity of 99.99% with surface area of 15×20 mm^2 and thickness of 0.30 mm.

The penetration depth of Xe^{20+} ions impacting on the iron target is about 0.36, 0.46, 0.55, 0.73, and 0.91 μm at the energies of 2.4, 3.0, 3.6, 4.8, and 6.0 MeV, respectively. This incidence range is smaller than the target thickness of 0.30 mm. Therefore, the target used in the present work can be considered as a thick target. The experimental X-ray production cross section can be derived from the X-ray yield using the well-known thick target formula[23]

$$\sigma_{\mathrm{X}}(E) = \frac{1}{n}\frac{\mathrm{d}Y}{\mathrm{d}E}\frac{\mathrm{d}E}{\mathrm{d}R} + \frac{\mu}{n}\frac{\cos\theta}{\cos\varphi}Y(E), \tag{1}$$

and that can be converted to inner-shell ionization cross section by using the fluorescence yield[6]

$$\sigma_i = \sigma_{\mathrm{X}}/\omega, \tag{2}$$

where n is the target atom density (atoms/g), μ is the mass absorption coefficient of the target for its own characteristic X-ray given by Hubbell,[24] θ is the incident angle to the normal direction of the target surface, φ is the observation angle to the target normal, $Y(E)$ is the X-ray yield per incident ion at impact energy E, $\mathrm{d}Y/\mathrm{d}E$ is extracted by calculating the differential coefficient on $Y(E)$ to E, and $\mathrm{d}E/\mathrm{d}R$ is the projectile stopping power calculated by SRIM.[25] The ionization cross section is σ_i for the i-shell electrons and ω is the fluorescence yield factor.

In the present work, the Fe K-shell X-ray yield per incident particle is calculated by

$$Y = \frac{N_{\mathrm{X}}}{N_{\mathrm{P}}\eta(\Omega/4\pi)}, \tag{3}$$

where N_{X} is the observed X-ray counts, which is extracted from the Gaussian fitting of the spectrum by a nonlinear curve fitting procedure, as shown in Fig. 1. The N_{P} is the total amount of incidence ions, which could be calculated by $N_{\mathrm{P}} = Q/(q \times 1.6 \times 10^{-19})$ (Q is the integral intensity of the projectile charge, q is the initial charge state of the projectile). η is the SDD efficiency, which is about 98% for Fe K_α and K_β X-rays. Ω is the solid angle of the detector. The total uncertainty of the yield is about 11% due to the statistics of the X-ray counts (5%) and the measurement of the incident ions number (10%). The uncertainty of the cross section mainly originates from the calculation of yield and the estimation of stopping power, which was estimated to be of the order of 22%.

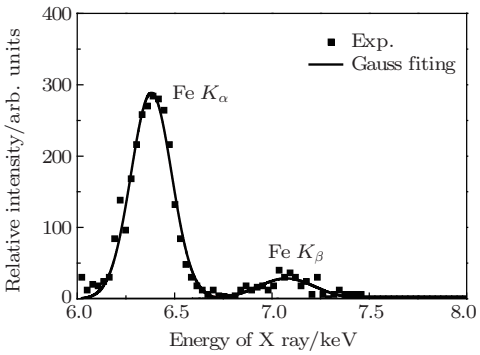


Fig. 1. Typical X-ray spectrum of iron induced by 6.0 MeV Xe^{20+} ions. Discrete square denotes the experimental result, solid line denotes the Gaussian fitting.

3. Results and discussion

In order to obtain the cross section, the Fe K-shell X-ray yield per incident ion was extracted from the X-ray spectra by Eq. (2). As shown in Fig. 2, the yield ranges from 10^{-8} to 10^{-6} and increases smoothly with increasing kinetic energy of the projectile.

Generally, during the process of highly charged ion–atom collisions, the K-shell fluorescence yield is different from the atomic data due to the multiple ionization of the L and M electrons. However, using the single-hole fluorescence, the yield should not bring additional uncertainties exceeding 10% for the ionization cross section calculation, because the K fluorescence yield should not change significantly unless the L-shell electrons are practically ionized.[26] This is impossible to occur in the solid target as verified by Tawara *et al.* that

the K-shell fluorescence yield is constant for a solid Si target for incident fluorine ions.[27] In the present work, there was no obvious shift of the X-ray. That means the L shell had no multiple vacancies during the K-shell X-ray emission. Therefore, we employ the single-hole fluorescence yield to calculate the K-shell ionization cross section. In view of the data of Krause,[28] the fluorescence yield used in our calculation is 0.340.

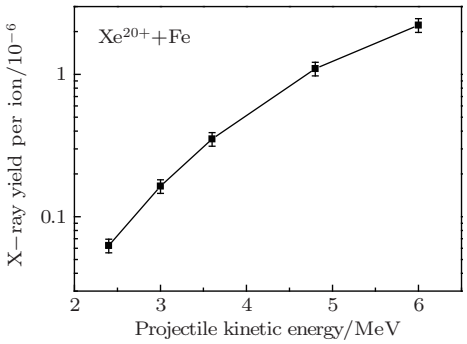


Fig. 2. The yield of Fe K-shell X-rays as a function of the projectile kinetic energy.

The K-shell ionization cross section of iron obtained by Eqs. (1) and (2) is presented in Fig. 3. It is about 0.23–2.72 barn (1 barn = 10^{-2} m^2) for the incident energy from 2.4 to 6.0 MeV, and increases smoothly with the increase in the scaled velocity V ($V = v_p/v_i$). The ECPSSR model,[29] which is based on plane-wave Born approximation and considers the effects such as energy loss (E) and Coulomb deflection (C) of the projectile, the modification of the atomic electron energy states through a perturbed stationary states model (PSS), and the adjustment of the electron mass due to the relativistic effects (R), is regarded as a the most excellent prediction to the inner-shell ionization by light ions. However, the present experimental result was underestimated by several magnitudes. Thus, we focus the BEA model to fit the results in this paper.

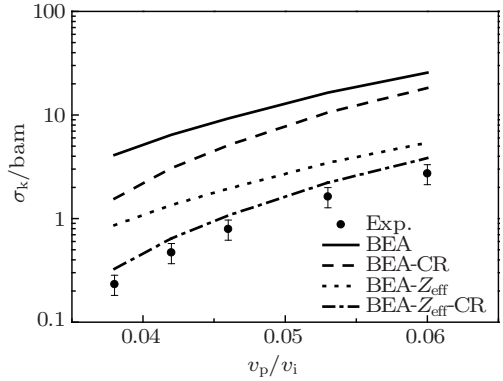


Fig. 3. Experimental Fe K-shell ionization cross section by Xe^{20+} ions, together with original BEA, BEA-CR, BEA-Z_{eff}, and BEA-Z_{eff}-CR models.

The binary-encounter-approximation (BEA) model,[30] which describes the inner-shell ionization as the classical collisions between the incident ions and the ionized electrons, calculates the ionization cross section for a definite energy transfer from the moving particles to the orbital electron of the target atoms. It is obvious in Fig. 3, the BEA prediction overestimates the experimental results by almost one order of magnitude and the deviation is large at the low kinetic energy of the projectile. The original model is independent of the projectile charge state and does not take into account the effect of projectile repulsion duo to the nuclear Coulomb field. Here we correct the simple BEA theory by taking into account the Coulomb repulsion to compare with our experimental results and attempt to discuss the effect of initial charge state to the inner-shell ionization of the target atom.

As discussed by Magno *et al*,[31] the effects of the Coulomb repulsion on the ionization cross section has two separated parts. One is the slowing-down of the projectile in the nuclear Coulomb field, which is important at the low incident energy. It presents the effective collision energy of the projectile. The other part arises from the change of the projectile trajectory duo to the Coulomb deflection. The correction formula of BEA by Coulomb repulsion (BEA-CR) can be written as[32]

$$\sigma_i(E_{p0}) = \sigma_i(E_p)\left[1/2 + 1/2\sqrt{E_p/E_{p0}}\right]^2, \tag{4}$$

where E_{p0} is the initial kinetic energy of the projectile, and $E_p = E_{p0} - Z_1(E_e + U)$ is the effective collision energy of the projectile. E_e and U are the kinetic energy and the binding energy of the electron, respectively. The cross section is $\sigma_i(E_p)$ for original BEA calculation given in a close form as[30]

$$\sigma_i^{BEA} = \left(\frac{NZ_1^2\sigma_0}{U^2}\right)G(V), \tag{5}$$

where N is the electron number for the i-shell, Z_1 is the projectile nuclear charge, $\sigma_0 = \pi e^4 = 6.5610^{-14}$ cm^2·eV^2, U is the electron binding energy, and $G(V)$ is a universal function of the scaled velocity $V = v_p/v_i$.

At low velocities, $v_p \ll v_i$, the highly charged heavy ions carrying their residual orbital electrons interact with the target atom in an asymmetrical collision system of $Z_1/Z_2 > 1$.[31] They act as ions or atoms rather than point charge particles, and the screening effect of the residual orbital electrons to the atomic nucleus cannot be ignored. Hence, in the case of low energy collisions, the projectile nuclear charge Z_1 must be replaced by the effective nuclear charge Z_{eff} for the cross section estimation in the classical BEA model. In the present work, we estimate the effective nuclear charge based on Slater's rule[33,34] ($Z_{eff} = Z_1 - \delta$, δ is the screening constant due to the shielding of the electrons between the nucleus and the electrons which is considered). The screening constant was estimated by taking into account the shielding of the residual electrons of the projectile with initial charge state. For Xe^{20+}, the initial electron configuration is $1s^22s^2p^63s^2p^6d^{10}4s^2p^4$, so

the screening constant is about 29.52. Correspondingly, the effective nuclear charge $Z_{\rm eff}$ is about 24.48.

The experimental Fe K-shell ionization cross sections are compared with theoretical calculations of BEA models, as shown in Fig. 3. Except for the original BEA model, the corrected BEA models, e.g., BEA-CR, which considers the Coulomb repulsion effect, BEA-$Z_{\rm eff}$ corrected by the effective nuclear charge $Z_{\rm eff}$ and BEA-$Z_{\rm eff}$-CR corrected by both the Coulomb repulsion and $Z_{\rm eff}$ are presented. The Coulomb repulsion correction has a significant effect at the lower collision velocity. For example, the correction is about 60% at the energy of 2.4 MeV, and about 30% at 6.0 MeV. With the single correction of Coulomb repulsion, the theoretical calculation almost cancels the difference of the deviation at various incident energies, but it still overestimates the experimental data by a factor of 7. Taking into account the single correction of effective nuclear charge, it reduces the classical BEA prediction by a factor of 2.2 and gives a closer representation of the experimental data than that of BEA-CR. Furthermore, after both corrections (CR and $Z_{\rm eff}$), although the theory overestimates experimental data in a small scale by factor of about 1.3, it presents a best prediction to the experimental trend and fits the experimental data better in the order of magnitude. This indicates that, in addition to the well-known Coulomb repulsion, the initial charge state of the projectile should also be considered to describe the inner-shell ionization in the slow, highly charged ions–atom collision.

Based on the above BEA-$Z_{\rm eff}$-CR theory, the X-ray emission induced by projectiles of different charge states should be different to a certain extent. Figure 4 displays the normalized X-ray spectra induced by Xenon ions with different charge states of 20+, 22+, 26+, and 30+. The relative BEA-$Z_{\rm eff}$-CR theoretical cross section and experimental yield for Fe K-shell X-ray are listed in Table 1. It can be seen that when the M shell of the projectile is closed ($Xe^{20+,22+,26+}$), the theoretical cross section ratio $\sigma_x^{(Xe^{q+})}/\sigma_x^{(Xe^{20+})}$ agrees quite well with that of the experimental yield $Y^{(Xe^{q+})}/Y^{(Xe^{20+})}$. Generally, the X-ray production cross section is proportional to the yield. It indicates that it is reasonable to correct the BEA model by effective nuclear charge $Z_{\rm eff}$ to simulate the Fe K-shell direct ionization by slow, highly charged xenon ions impact.

However, when the projectile has initial M-shell vacancies (Xe^{30+}), the Fe K-shell X-ray emission shows a large enhancement as shown in Fig. 4, which cannot be predicted by the BEA-$Z_{\rm eff}$-CR theory. We think molecular-orbital promotion should also be considered in the inner-shell ionization process for such energy range and projectile combination, except for direct ionization. In the Xe^{30+}+Fe collision system, the inner-shell vacancies are formed in the highly promoted MO's state ($3d\sigma$) at a very short inter-nuclear distance, and the Xe L-shell vacancies ($3d\sigma$) can be shared with the Fe K-shell ($2p\sigma$) via level crossing. If the ground state energy of Xe^{30+} and Fe atom was employed, about 14% of Xe L-shell vacancies will be transferred to Fe K-shell by a rough estimation,[35,36] which would result in a substantial increase of Fe K-shell X-ray emission. Meanwhile, due to the electron transfer, the number of Xe L-shell vacancies filled by X-ray emission may be reduced. Compared to Fig. 4, L-shell X-ray yield of Xe^{30+} is smaller than that of Xe^{20+} by a factor of 2.20, which is larger than the BEA estimation of 1.62. Here again we emphasize the fact that, when the highly charged ions enter into the solid target, the projectile will reach equilibrium charge state on a scale of femtosecond, and the energy gap between Xe L-shell and Fe K-shell will be enlarged as the initial charge state decreases to the equilibrium charge state, which leads to a rapid decrease of vacancy transfer. In order to explore the contribution of the vacancy transfer, a further experiment with very thin foil targets should be done in the future.

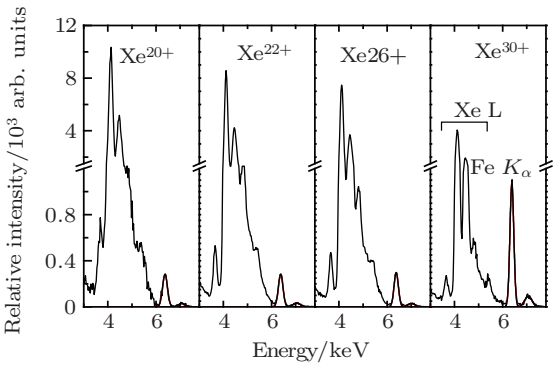


Fig. 4. Normalized X-ray spectra of Fe produced by 5.0 MeV Xe^{q+} (q = 20, 22, 26, and 30) ions impacting on solid Fe target, which was normalized by the incident ions number.

Table 1. Effective nuclear charge for xenon ions with different charge states calculated by Slater's rule,[32] theoretical cross section and experimental yield of Fe K-shell X-ray produced by Xe^{q+} ions, and the corresponding ratio. $\sigma_x^{(Xe^{q+})}$ is the theoretical Fe K-shell X-ray production cross section induced by Xe^{q+} ions, and $Y_{\rm Fe}^{(Xe^{q+})}$ is the experimental Fe K-shell X-ray yield per ions by Xe^{q+} ions.

Charge state	$Z_{\rm eff}$	$\sigma_x^{\rm BEA-CR-Z_{eff}}$/barn	$Y_{\rm EXP}/10^{-6}$	$\sigma_x^{(Xe^{q+})}/\sigma_x^{(Xe^{20+})}$	$Y^{(Xe^{q+})}/Y^{(Xe^{20+})}$
20+	24.48	0.82	1.29±0.14	1	1
22+	25.08	0.86	1.38±0.16	1.05	1.07±0.12
26+	27.24	1.02	1.54±0.17	1.24	1.20±0.13
30+	33.84	1.57	4.89±0.34	1.91	3.79±0.27

4. Conclusion

We have measured the Fe K-shell ionization cross sections by 2.4–6.0 MeV Xe^{20+} impacting and compared the X-ray emission induced by 5 MeV xenon ions with different charge states. By comparing the experimental results with the BEA predictions, it was found that the initial charge state of the projectile should be considered in the slow, highly charged ions–solid collisions. Effective nuclear charge $Z_{\rm eff}$ correction for the BEA model is reasonable to describe the Fe K-shell ionization induced by slow, highly charged xenon ions with no initial M shell. The BEA model corrected by both the Coulomb repulsion and the effective nuclear charge presents the best agreement to the experimental cross section. However, when the M shell of xenon is opened, the BEA theory cannot give a reasonable description of the experimental results, and the mechanism of electron transfer should be taken into account for inner-shell ionization as well.

Acknowledgment

The authors sincerely acknowledge the technical support from the LAPECR2 group.

References

[1] Arnau A, Aumayr F, Echenique P M, Grether M, Heiland W, Limburg J, Morgenstern R, Roncin P, Schippers S, Schuch R, Stolterfohf N, Varga P, Zouros T J M and Winter H P 1997 *Surf. Sci. Rep.* **27** 113
[2] Schenkel T, Hamza A V, Barnes A V and Scheider D H 1999 *Prog. Surf. Sci.* **61** 23
[3] Phinney L C, Lapicki G, Weathers D L, Naab F U, Duggan J L and McDaniel F D 2012 *J. Phys. B* **45** 035205
[4] Phinumber Azordegan A R, Sun H L, Yu Y C, Duggan J L, McDaniel F D, Lin E K, Wang C W and Lapicki G 2012 *J Phys. B* **45** 035205
[5] Reyes-Herrera J and Miranda J 2009 *Nucl. Instr. Melth. B* **267** 1767
[6] Miranda J, Lucio O G and Lugo-Licona M F 2007 *Rev. Mex. Fis. S* **53** 29
[7] Burgdorfer J, Lerner P and Meyer F 1991 *Phys. Rev. A* **44** 5674
[8] Lugo-Licona M and Miranda J 2004 *Nucl. Instr. Met. B* **219** 289
[9] Merzbacher E and Lewis H 1958 *Handbuüch der Physik* **34** 166
[10] Halpern A M and Law J 1973 *Phys. Rev. Lett.* **31** 4
[11] Fano U and Lichten W 1965 *Phys. Rev. Lett.* **14** 627
[12] Madison D H and Merzbacher E 1975 *in Atomic Inner-Shell Processes* (edited by Crasemann B) (New York: Academic) (vol. 1) pp. 1–72
[13] Zhao Y T, Xiao G Q, Zhang X A, Yang Z H, Zhan W L, Chen X M and Li F L 2006 *Nucl. Instr. Melth. B* **245** 72
[14] Chen X M, Shao J X, Yang Z H, Zhang H Q, Cui Y, Xu X, Xiao G Q, Zhao Y T, Zhang X A and Zhang Y P 2007 *Eur. Phys. J. D* **41** 281
[15] Zhang H, Chen X, Yang Z, Xu J, Cui Y, Shao J, Zhang X, Zhao Y, Zhang Y and Xiao G 2010 *Nucl. Instr. Melth. B* **268** 1564
[16] Hattass M, Schenkel T, Hamza A V, Barnes A V, Newman M W, McDonald J W, Niedermayr T R, Machicoane G A and Scheider D H 1999 *Phys. Rev. Lett.* **82** 4795
[17] Winecki S, Cocke C L, Fry D and Stockli M P 1996 *Phys. Rev. A* **53** 4228
[18] Winecki S, Stockli M P and Cocke C L 1997 *Phys. Rev. A* **55** 4310
[19] Schenkel T, Briere M A, Barnes A V, Hamza A V, Bethge K, Schmidt-Boecking H and Scheider D H 1997 *Phys. Rev. Lett.* **79** 2030
[20] Herrmann R, Cocke C L, Ullrich J, Hagmann S, Stoeckli M and Schmidt-Boecking H 1994 *Phys. Rev. A* **50** 1435
[21] Hoffmann D H H, Jacoby J, Laux W, Magistris M, Boggasch E, Spiller P, Stockl C, Tauschwitz A, Weyrich K, Chabot M and Gards D 1994 *Nucl. Instr. Melth. B* **90** 1
[22] Wang X, Zhao Y T, Cheng R, Zhou X M, Xu G, Sun Y B, Lei Y, Wang Y Y, Ren J R, Yu Y, Li Y F, Zhang X A, Li Y Z, Liang C G and Xiao G Q 2012 *Phys. Lett. A* **376** 1197
[23] Garcia J D, Fortner R J and Kavanagh T M 1973 *Rev. Mod. Phys.* **45** 111
[24] Hubbell J H *et al.* 1969 *Lawrence Livermore National Laboratory Report* UCRL-50174
[25] http://www.srim.org/
[26] Meyerhof W E, Robert A, Saylor T K, Lazarus S M and Little A 1976 *Phys. Rev. A* **14** 1653
[27] Tawara H, Richard P, Gray T J, Newcomb J, Jamison K A, Schmiedekamp C and Hall J M 1978 *Phys. Rev. A* **18** 1373
[28] Krause M O 1979 *J. Phys. Chem. Ref.* **8** 307
[29] Lapicki G and McDaniel F D 1981 *Phys. Rev. A* **23** 975
[30] McGuire J H and Richards P 1973 *Phys. Rev. A* **8** 1374
[31] Magon C, Milazzo M, Pizzi C, Porro F, Rota A and Riccobono G 1979 *Nuovo Cimento A* **54** 277
[32] Basbas G, Brandt W and Laubert R 1973 *Phys. Rev. A* **7** 983
[33] Slater J C 1930 *Phys. Rev.* **36** 57
[34] Liu S Z 1986 *Atomic Structure and Chemical Periodic System of Elements* (Beijing: Science and Technology Press) p. 108
[35] Meyerhof W E, Anholt R, Eichler J and Salop A 1978 *Phys. Rev. A* **17** 108
[36] Nikitin E E 1970 *Adv. Quantum Chem.* **5** 135